ORIGINAL RESEARCH

Imaging Pattern of Diffuse Intrapulmonary Metastases in Lung Cancer Was Associated with Poor Prognosis to Epidermal Growth Factor Receptor Inhibitors

Yang Fu[1]
Yuan Tang[2]
Yue Zheng[1]
Yue-Yun Chen[1]
Ye Hong[1]
Pei-Pei Wang [ID][1]
Qing Li[1]
Ting Liu [ID][1]
Zhen-Yu Ding[1]

[1]Department of Biotherapy, Cancer Center, West China Hospital, West China Medical School, State Key Laboratory of Biotherapy, Sichuan University, Chengdu, People's Republic of China; [2]Department of Pathology, West China Hospital, West China Medical School, Sichuan University, Chengdu, People's Republic of China

Background: Epidermal growth factor receptor (EGFR) mutations are more frequently seen in miliary intrapulmonary metastases than EGFR wild-type non-small cell lung cancer (NSCLC). Also, small-scale retrospective studies showed that patients harboring EGFR mutation with miliary pulmonary metastases had a worse prognosis. This study aimed to explore the impact of imaging patterns on the outcomes of EGFR tyrosine kinase inhibitor (TKI) treatment.

Methods: A cohort of treatment-naive NSCLC patients harboring EGFR mutation with intrapulmonary metastases who were prescribed with TKI were enrolled. The demographic feature, clinical outcome, and CT imaging of each patient were reviewed and analyzed.

Results: A cohort of 174 patients were enrolled. Five intrapulmonary patterns of imaging were recognized: solid nodular, ground-glass nodular, miliary, multiple uniform nodular, and not otherwise specified. Among them, miliary and multiple uniform nodular patterns had similar poor prognosis, and, therefore, were combined as diffuse group. A worse PFS (9.0 mon, 95% CI: 8.0–10.0 mon) was observed compared with the rest (non-diffuse group, 13.3 mon, 95% CI: 10.2–16.4 mon, $p<0.001$, HR=0.49). The objective response rates (ORR) between the two groups were 76.8% and 84.1%, respectively, with no significant difference ($p = 0.474$). The OS of the diffuse and the non-diffuse group were 25.6 mon (95% CI 21.9–29.3 mon) and 35.0 mon (95% CI: 27.5–42.5, $p = 0.01$, HR= 0.59). Organs like bone ($p=0.167$), liver ($p=0.513$), and adrenal gland ($p=0.375$) were involved in similar frequencies in both groups. However, brain ($p=0.070$) and leptomeningeal ($p=0.078$) metastases were less common in the non-diffuse group with marginally statistical significance. The 2 groups contained similar missense mutations, and gene amplification was more common in the non-diffuse group.

Conclusion: Patients with diffuse intrapulmonary metastases had inferior outcomes after TKI treatment. More aggressive treatments might be warranted for these patients.

Keywords: epidermal growth factor receptor, EGFR, tyrosine kinase inhibitor, TKI, CT imaging, outcome, genetic aberration

Correspondence: Zhen-Yu Ding
Department of Biotherapy, Cancer Center, West China Hospital, West China Medical School, State Key Laboratory of Biotherapy, Sichuan University, Chengdu 610041, People's Republic of China
Tel +86 028 8542 2562
Fax +86 028 8516 4059
Email dingzhenyu@scu.edu.cn

Introduction

Lung cancer is the leading cause of cancer-related death in the world.[1] For those with metastatic diseases, the 5-year survival is around 5%. The prognosis of patients suffering from advanced non-small cell lung cancer (NSCLC) is improved with the advent of epidermal growth factor receptor (EGFR) targeted therapy,

especially for those harboring EGFR mutation. EGFR-tyrosine kinase inhibitors (TKIs) have demonstrated superior efficacy over traditional chemotherapy in these patients, and achieved better progression-free survival (PFS).[2–4] Nowadays, EGFR TKI has been recommended as the standard-of-care. Although EGFR mutation largely dictates the sensitivity to TKI, clinical response varies. We still need to explore additional factors contributing to the efficacy of EGFR-TKI.[5,6]

The lung is frequently a metastatic organ of NSCLC. Computed tomography (CT) is widely used in clinic to evaluate lung cancer patients. According to imaging characteristics, several different patterns including multiple intrapulmonary nodules, pleural effusions and enlarged lymph nodes were presented.[7,8] A few studies have been carried out to investigate the imaging features of NSCLC with EGFR mutations. EGFR mutations are more frequently seen in miliary intrapulmonary metastases than EGFR wild-type NSCLC.[9–11] Also, small-scale retrospective studies showed that patients harboring EGFR mutation with miliary pulmonary metastases had a worse prognosis. However, no underlying mechanisms were provided. We hypothesized the imaging manifestation was determined by the intrinsic genomic aberration of tumor cells, and was closely related to the therapeutic outcomes. Our study aimed to explore the impact of imaging patterns on the outcomes of EGFR TKI treatment. A cohort of NSCLC patients harboring EGFR mutation were enrolled and the data were analyzed.

Methods
Patients
This retrospective, observational study was conducted in patients screened through the Hospital Information System from January 2012 to January 2019. Patients were pathologically confirmed, metastatic, treatment-naive NSCLC patients harboring EGFR mutation who were prescribed with EGFR-TKI. Patients must have intrapulmonary metastases on CT imaging. Those treated with TKI combined with chemotherapy, either synchronous or intercalated, or mixed small-cell lung cancer were excluded.

Treatment Protocol
Gefitinib (250 mg, AstraZeneca plc, London, UK) and erlotinib (150 mg, Hoffman La-Roche Ltd., Basel, Switzerland) were both orally taken once per day, and icotinib (125 mg, Beta, China) was medicated 3 times a day. Treatment continued until disease progression, or unacceptable toxicity, or death from any cause. The selection of each drug was determined by the treating physicians' discretion.

Genetic Testing
Genetic testing was performed on tumor tissues. EGFR mutation was detected by ARMS using a commercially available kit (AmoyDx, Shameng, China) in our domestic, College of American Pathologists-certified lab in authors' hospital. Tumor content was assessed by board-certified pathologists using hematoxylin and eosin staining. All specimens contained more than 10% tumor content. DNA was extracted using the QIAamp DNA mini kit (Qiagen). In some patients, comprehensive genomic profiling was performed by Next Generation Sequencing (NGS) with 56 cancer-related gene panel covering the whole exons of EGFR gene at a mean coverage depth of >800X. The genomic alterations including single base substitution, insertions/deletions, copy number variations, as well as gene rearrangement and fusions were assessed.

Imaging
A whole-chest CT scan, ranging from the level of the superior aperture of the thorax to the top of the diaphragm, was performed with one breath-hold. The images were reviewed using lung window settings (width: 1500 HU, level: −600HU). The thickness and interval of the layer were 1 mm. CT images were independently reviewed under the supervision of a radiologist who was kept blind to the clinical data. Differences in their interpretations were resolved by discussion.

Outcome Measures
Tumors were assessed every 2 months radiographically, including CT of the chest and upper abdomen, magnetic resonance imaging of the head, and bone scintigraphy. Tumor response was evaluated as complete response (CR), partial response (PR), stable disease (SD), or progression disease (PD), according to RECIST 1.1. The progression-free survival (PFS) was defined as the duration from the initiation of the therapy to the date of disease progression, intolerable side effects, or death from any cause. The overall survival (OS) was defined as the duration from the initiation of the therapy to the date of death from any cause. The ethical committee of authors' university reviewed and approved the study concept and the

study was performed in accordance with the Declaration of Helsinki.

Data Analysis

Statistical analysis was performed using SPSS version 22.0 (IBM Corporation, Armonk, NY, USA) and the multivariate analysis was output by GraphPad Prism 7.00 (GraphPad Software, Inc., La Jolla, CA, USA). The quantitative were compared using chi-square test and Fischer's exact test according to Cochran's rule. The Kaplan–Meier curve was used to compare survival. Multi-variate analysis was done by using a Cox proportional hazard model. All P-values were based on a two-tailed hypothesis, and statistical significance was assumed if p < 0.05.

Results

Imaging Patterns

To summarize the imaging patterns of lung metastases, we reviewed CT scans of a cohort of NSCLC patients harboring EGFR mutation. This cohort was screened from our database of lung cancer registration infrastructure. Totally 3389 patients were screened, and 174 patients were enrolled (Figure 1). The imaging could be divided into 5 patterns: solid nodular, ground-glass nodular, miliary, multiple uniform nodular, and not otherwise specified (Figure 2A and B). Whether multiple ground glass nodules were due to synchronous primaries or metastatic lesions was a clinical dilemma. Gaikwad et al described aerogenous metastases in lung adenocarcinoma, with CT appearance of synchronous primaries.[12] Also, Li et al reported clinical evidence of multiple ground glass nodules attributed to metastasis, but not synchronous primaries.[13] The determination of primary or metastatic lesion depended on invasive surgical resection or biopsy, which was not possible for our patients with extensive intra- and extra-pulmonary metastases. In our study, most patients with ground-glass nodular metastases had simultaneous extrapulmonary (16/ 18, 88.9%) or lymph node metastases (15/18, 83.3%). These nodules were most likely metastatic. Of notice, miliary intrapulmonary metastases were defined as uncountable, round, randomly distributed, uniformly dense, small nodules in the lung with a diameter of 1–5 mm. Multiple uniform nodular intrapulmonary metastases had similar imaging presentation, however with a larger diameter of 5 mm to 2 cm. Cancerous lymphangitis were excluded. Among them, solid nodular metastases pattern was the most common.

Worse Outcomes of the Diffuse Group

Among our patients, the average age was 58.4 years. Gefitinib, erlotinib, or icotinib were medicated in 104 (59.8%), 25 (14.3%), and 45 (25.9%) patients, respectively. 171 (98.3%) patients had classic mutations (exon19 deletion or exon21 *L858R* missense mutation), and 3 (1.7%) patients had non-classic mutations such as *L861Q, S768I* point mutation. At the time of diagnosis, 123 (70.7%) patients had both extra- and intra-pulmonary metastases, while 51 (29.3%) patients had only intrapulmonary metastases. The overall PFS and OS of the population were 10.8 months (95% CI 9.5 −11.0 mon) and 28.2 mon (95% CI 25.1–35.2 mon, Figure 3A).

To explore the possible relationship between therapeutic efficacy and imaging patterns, PFS curves of different patterns were constructed and compared. And we found those with miliary or multiple uniform nodular metastases had comparable PFS after TKI treatment. We combined these 2 patterns and referred them as diffuse group. And we got 86 and 88 patients in the diffuse and non-diffuse intrapulmonary metastases group each. Both groups had comparable demographic features (Table 1).

Worse PFS of the diffuse group (9.0 mon, 95% CI: 8.0–10.0 mon) was observed than that of the non-diffuse group (13.3 mon, 95% CI: 10.2–16.4 mon, p<0.001, HR=0.49, Figure 3B). The objective response rates (ORR) between the two groups were 76.8% and 84.1%, respectively, with no significant difference (p = 0.474). The OS of the diffuse and the non-diffuse group were 25.6 mon (95% CI 21.9–29.3 mon) and 35.0 mon (95% CI: 27.5–42.5, p = 0.01, HR=0.59, Figure 3C). Our patients all had metastatic diseases (at least M1a), with similar poor prognosis irrespective of their T stages. We found in our non-diffuse group, patients with lesions in the same lobe (stage T2, n=11), or other lobe of ipsilateral lung (T4, n=26), or contralateral lung (n=5) had similar survival (30.9, 44.7, and NA due to few patients, p=0.69).

The Worse Efficacy Could Not Be Rescued by Osimertinib

To confirm the negative impact of diffuse metastases on PFS, we performed a COX multivariate analysis. In this regressive analysis, after exclusion of influences of age, gender, smoking, performance status, EGFR mutation type, multiple brain metastases and
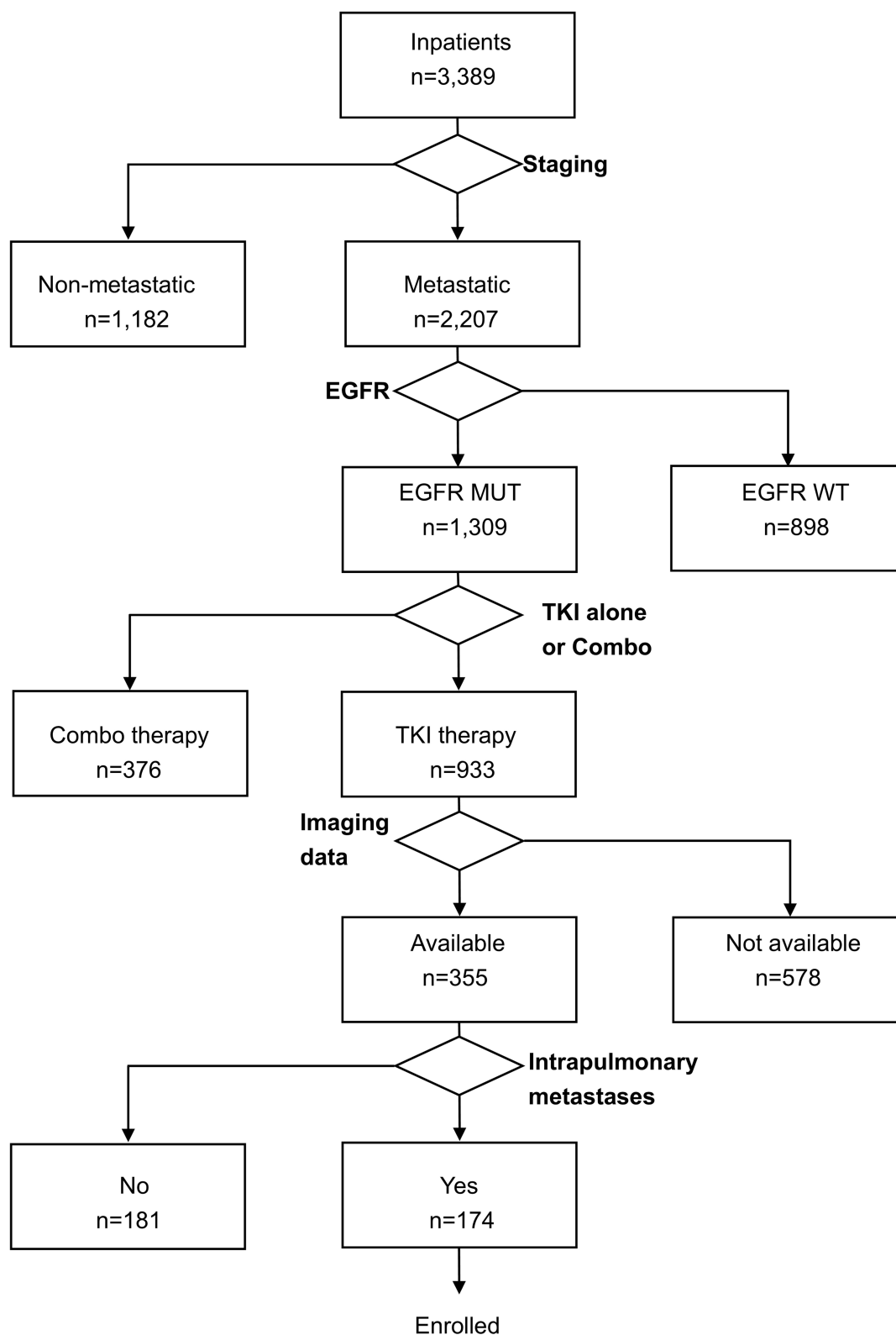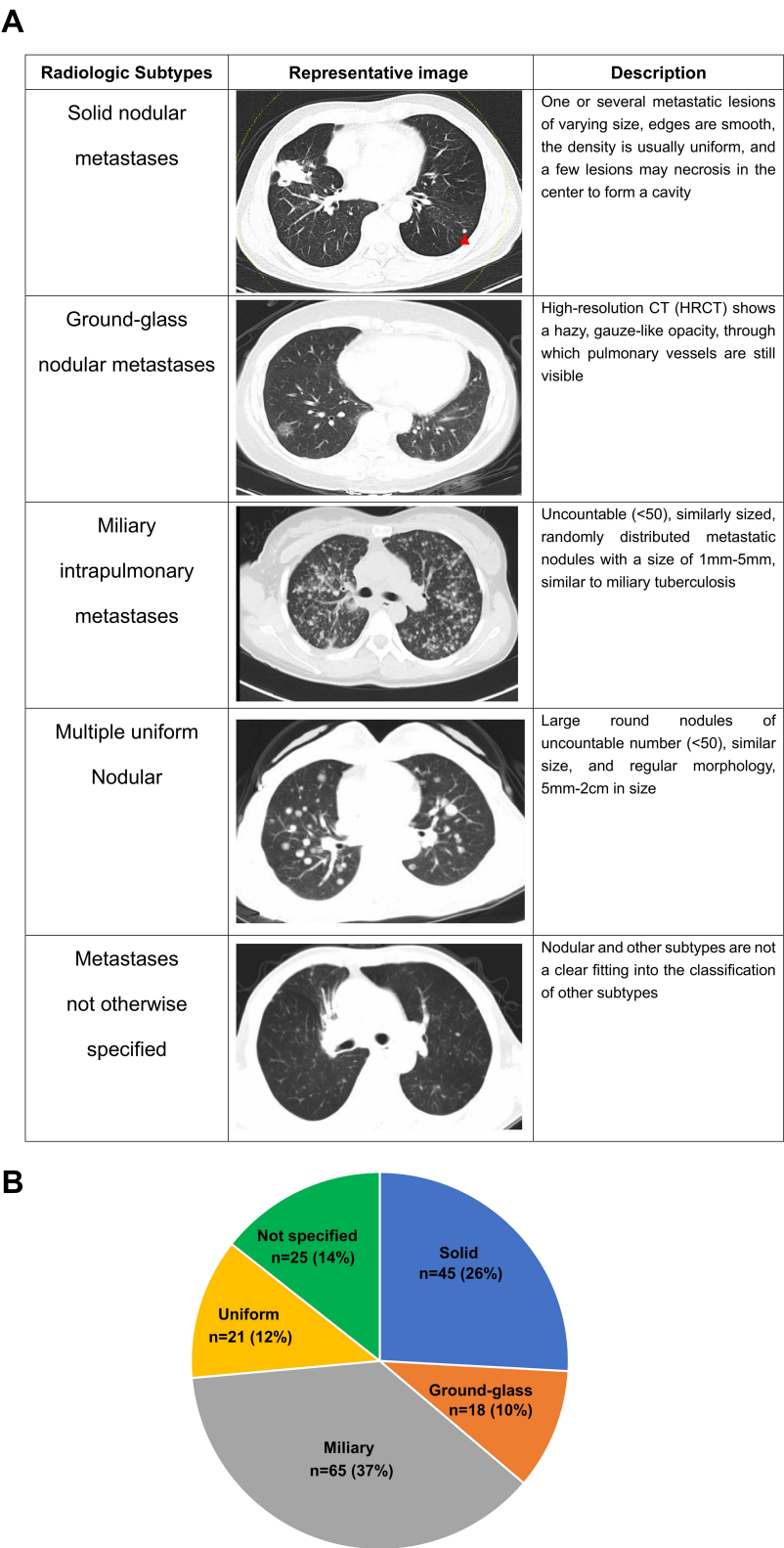
Figure 1 Flow chart of patients screening. MUT: mutation, WT: wild-type.

leptomeningeal metastases, diffuse metastases remained as an independent inferior predicator of TKI treatment (Figure 3D).

Twenty patients in the diffuse group and 16 patients in the non-diffuse group switched to osimertinib after failure of the first generation TKIs. PFS of the two groups were

A

Radiologic Subtypes	Representative image	Description
Solid nodular metastases		One or several metastatic lesions of varying size, edges are smooth, the density is usually uniform, and a few lesions may necrosis in the center to form a cavity
Ground-glass nodular metastases		High-resolution CT (HRCT) shows a hazy, gauze-like opacity, through which pulmonary vessels are still visible
Miliary intrapulmonary metastases		Uncountable (<50), similarly sized, randomly distributed metastatic nodules with a size of 1mm-5mm, similar to miliary tuberculosis
Multiple uniform Nodular		Large round nodules of uncountable number (<50), similar size, and regular morphology, 5mm-2cm in size
Metastases not otherwise specified		Nodular and other subtypes are not a clear fitting into the classification of other subtypes

B

Figure 2 Five patterns of radiologic manifestations of intrapulmonary metastases (**A**). Number and percentage of patients in each pattern (**B**). Red arrow represented the contralateral metastasis.
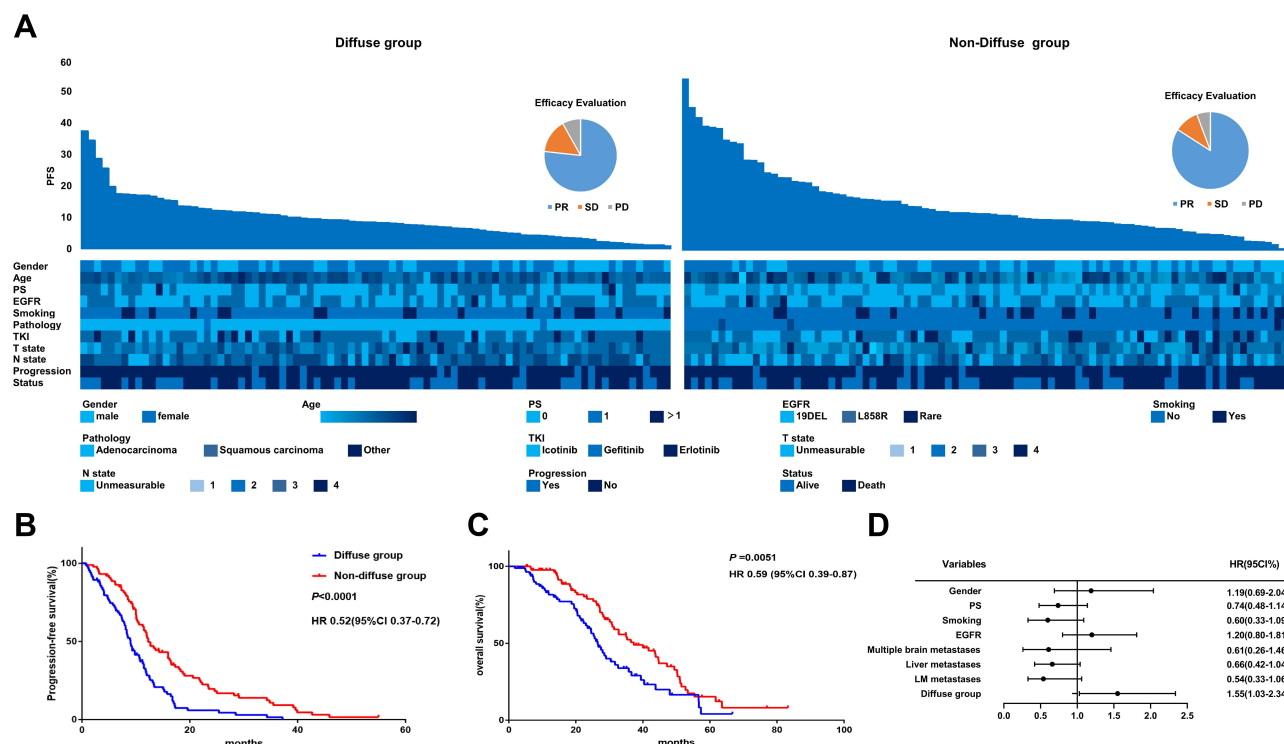
Figure 3 The PFS of each patient in either diffuse and non-diffuse group was presented, together with each patient's characteristics including gender, age, EGFR mutation, smoking history, pathology, TKI, ECOG, T state, N state status, PFS, and ORR (**A**). Diffuse group showed inferior PFS (**B**) and OS than non-diffuse group (**C**). Imaging pattern was an independent factor related to PFS (**D**).

5.2 mon (95% CI: 4.6–9.9 mon) and 14.6 mon (95% CI: 13.0–19.8 mon). PFS of the diffuse group was still significantly shorter (p < 0.001, HR=0.36, Figure 4A).

A total of 9 patients received immune checkpoint inhibitors (ICIs) as salvage therapy. Among them, 7 patients were prescribed with chemotherapy and ICIs combo therapy, and 2 patients were treated with ICIs alone. All patients in the diffuse group had progressed disease, and 4/5 of them died. While in the non-diffuse group, 3/4 patients kept alive, and 2 patients remained in ICI therapy with PR (Figure 4B).

The Diffuse Group Was Prone to Diffuse Metastases in Multiple Organs

To evaluate the metastatic potential of the diffuse group, we analyzed the metastatic organs. The most common metastatic organs were bone (65.1%), brain (53.5%), liver (20.9%), leptomeningeal (19.8%), and adrenal gland (11.6%, Figure 5A). Bone (54.5%, p=0.167), liver (17.0%, p=0.513), and adrenal gland (13.6%, p=0.375) were involved in similar frequencies when compared to those of the non-diffuse group. However, brain (39.8%, p=0.070) and leptomeningeal (10.2%, p=0.078) metastases were less common in the non-

diffuse group (Figure 5B) with marginally statistical significance.

The uncountable, round, randomly distributed lesions were observed in other organs as well (Figure 5C). When countering these foci, more patients in the diffuse group have diffuse metastases in brain (n=9 and 1), liver (n=4 and 2), and bone (n=6 and 2) than those in the non-diffuse group. Patients with diffuse intrapulmonary metastasis were more susceptible to diffuse metastases in other organs (p=0.009, Figure 5D).

Genetic Aberration of the Diffuse Group

We collected the targeted sequencing data from a panel consisting of 56 genes from both groups. This cohort with available genetic data (n=21 in the diffuse group, and n=40 in the non-diffuse group) had no significant differences in the number of missense mutations in the two groups. But amplifications were more common in the non-diffuse group (Figure 6A and B).
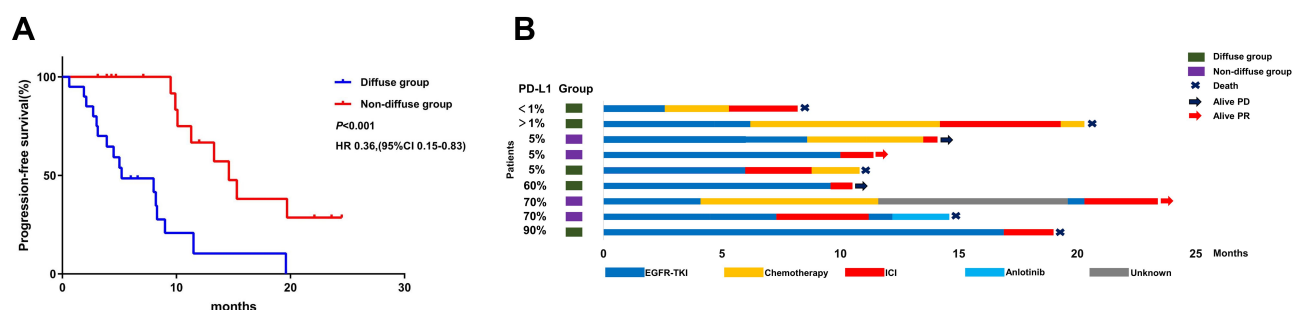
Discussion

In this paper, we described the imaging presentation of NSCLC harboring EGFR mutation as one of the 5

Table 1 Clinical characteristics of NSCLC patients with Intrapulmonary metastases at initial diagnosis

Characteristics	Diffuse Group	Non-Diffuse Group	Total	P-value
Age-yr ≥65 <65	 26(30.2%) 60(69.8%)	 34(38.6%) 54(61.4%)	 60(34.5%) 114(65.5%)	0.180
Gender Male Female	 32(37.2%) 54(62.8%)	 37(42.0%) 51(58%)	 69(39.7%) 105(60.3%)	0.539
ECOG 0 ≥1	 50(58.1%) 36(41.9%)	 52(59.0%) 36(41.0%)	 102(58.6%) 72(41.4%)	0.899
Smoking history Yes No	 18(20.9%) 68(79.1%)	 20(22.7%) 68(77.3%)	 38(21.8%) 136(78.2%)	0.855
Histologic Adenocarcinoma Others	 84(97.7%) 2(2.3%)	 83(94.3%) 5(5.7%)	 167(96.0%) 7(4.0%)	0.644
EGFR mutations Classic mutation Rare mutation	 85(98.8%) 1(1.2%)	 86(97.7%) 2(2.3%)	 171(98.3%) 3(1.7%)	0.574
TKI Icotinib Gefitinib Erlotinib	 19(22.1%) 55(63.9%) 12(14.0%)	 26(29.5%) 49(55.7%) 13(14.8%)	 45(25.9%) 104(59.8%) 25(14.3%)	0.495
Extra-pulmonary metastases Yes No	 66(76.7%) 20(23.3%)	 57(64.8%) 31(35.2%)	 123(70.7%) 51(29.3%)	0.097

patterns: solid nodular, ground-glass nodular, miliary, multiple uniform nodular, and not otherwise specified. The diffuse intrapulmonary metastases including miliary and multiple uniform nodular had a worse PFS and OS after TKI treatment. In addition, the diffuse group was prone to diffuse metastases in other organs, and contained less gene amplification.

The relationship between imaging presentation and EGFR mutation was noticed before. Miliary intrapulmonary metastases is a special type of NSCLC, with an incidence of approximately 2%. Most of the pathological types are adenocarcinoma, which is considered to be the result of blood circulation in the lung.[7,8,14] EGFR mutations are more frequently seen in miliary intrapulmonary metastases than
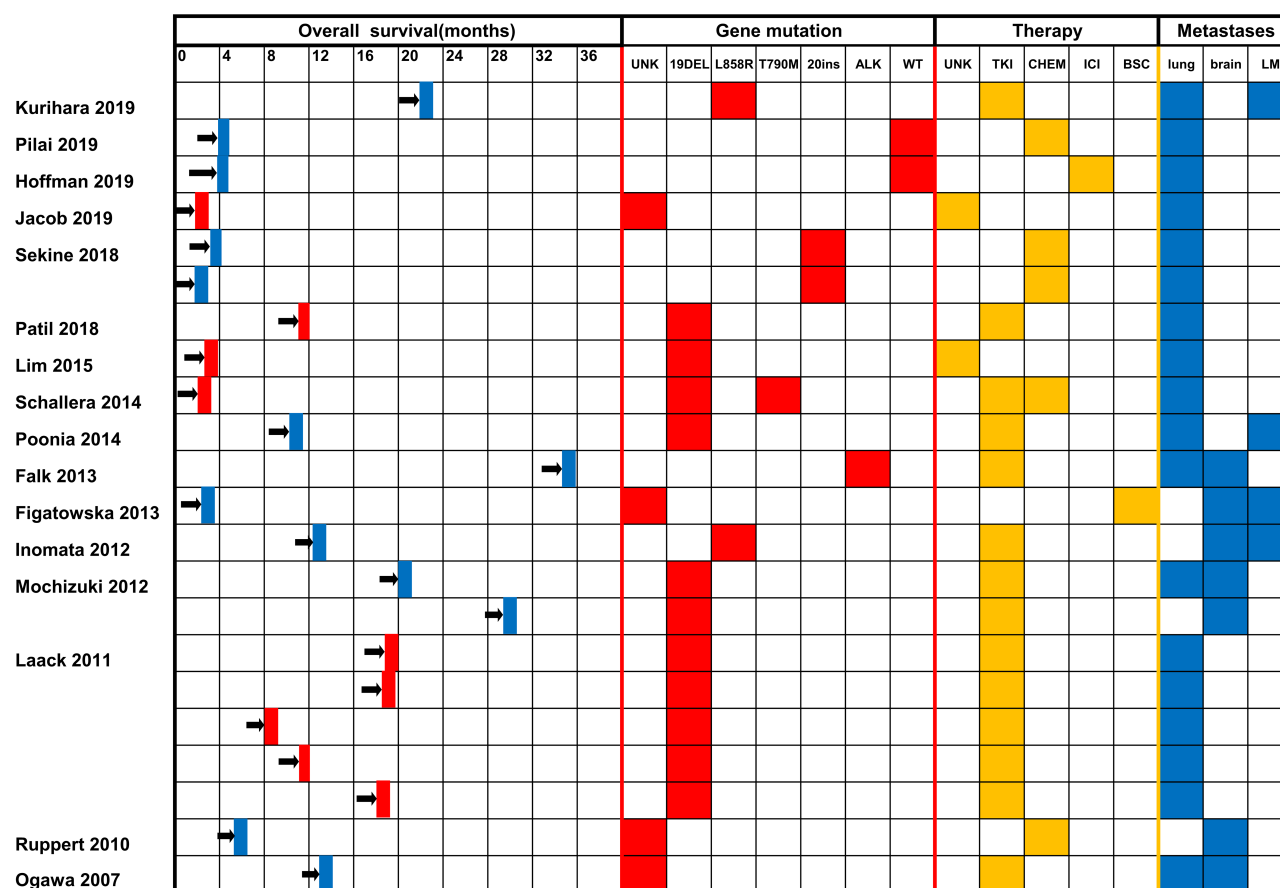

Figure 4 Diffuse group had shorter PFS when treated with osimertinib (**A**). Nine patients received ICIs as salvage therapy. Clinical event timeline of each patient (**B**).

Figure 5 Summary of metastases sites in the diffuse groups (**A**). Organs were involved in similar frequency between 2 groups, except brain and leptomeningeal (**B**). A typical case of miliary intrapulmonary metastases, together with diffuse metastases of bone and brain (**C**). Diffuse group had higher frequencies of diffuse metastases in other organs. Each dot represented a patient (**D**).

EGFR wild-type NSCLC.[12] However, whether the imaging pattern was related to TKI treatment efficacy remained largely overlooked. Previously, Wu et al reported a median PFS for chemotherapy in patients with miliary intrapulmonary metastases was only 2.9 months.[14] With the advent of TKI, Kim et al and Okuma et al proposed that the prognosis of miliary intrapulmonary metastases of EGFR mutant was worse than that of non-miliary metastases.[7,8] But this point was not supported by Hsu et al.[11] The small sample size of miliary intrapulmonary metastases enrolled in these studies might contribute to the seemly paradoxical conclusions.[7,8,11] This current study revealed shorter PFS, OS, and numerically lower ORR, in this group of patients. We also found the inferior response of this group could not be reversed by osimertinib or ICIs. Maybe treatment unresponsiveness is an intrinsic feature related to the diffuse intrapulmonary metastases group.

The therapeutic efficacy of the diffuse metastases pattern was reported in a previous small-scale retrospective study[17] and numerous anecdotal cases reports.[20–33] Here we made a brief summary of these case reports (Figure 7).

All the reports consistently showed the unsatisfactory outcomes irrespective of variant treatments. Our results were strongly supported by these reports.

Previous reports described the imaging features of miliary intrapulmonary metastases as uncountable, round, randomly distributed, uniformly dense, small nodules with a diameter < 5 mm.[14] In our series of patients, we found another form of multiple metastases similar to miliary form, with a larger size (5 mm–2 cm in diameter). This pattern of imaging was ignored before and excluded in previous studies by Kim, Okuma, and Hsu et al.[7,8,11] In addition, we found this imaging pattern had similar poor clinical responses to TKI treatment as that of miliary metastases. We later combined these two patterns and referred them as diffuse intrapulmonary metastases.

This study also tried to observe the unique biological behavior of this diffused intrapulmonary metastases. We found organs like bone, liver, and adrenal gland were similarly involved in both diffuse and non-diffuse group. But brain and leptomeningeal were more susceptible in the diffuse group, both of which were notorious for poor

Figure 6 Genetic aberrations in two groups (**A**). Both groups had similar point mutations, but gene amplification was less common in the diffuse group (**B**).

prognosis.[16–19] We also found the frequencies of missense mutations in the two groups were similar, but gene amplification was less observed in the diffuse

group. Whether these genetic aberrations contributed to the development of the different imaging patterns remained largely unknown, but there is evidence the

Figure 7 Summary of literature on the outcomes of lung cancer patients with diffused intrapulmonary metastases. The arrow indicated the advent of event. The blue bar indicated the death of the patient, while the red bar meant the censored data.
Abbreviations: UNK, unknown; 19DEL, EGFR exon 19 deletion; L858R, EGFR exon 21 L858R missense mutation; T790M, T790M mutation; 20ins, EGFR exon20 insertion; WT, wild-type; CHEM, chemotherapy; ICI, immunotherapy; BSC, best supportive care; lung, diffuse intrapulmonary metastases; brain, diffuse brain metastases; LM, leptomeningeal metastases.

genomic heterogeneity related to the clinical unresponsiveness to treatments.[35–38]

The current study had its pitfalls. Firstly, all the patients were enrolled from a single institute, which might introduce possible bias. Secondly, genetic profiles were available in only a small fraction of our patients. This was because NGS targeted sequencing platform was not available before the year 2017. Those without information of their genetic mutation landscape would possibly confound the current analysis. Thirdly, the comparison of the diffuse and non-diffuse group was not based on randomization. We are continuing to accumulate cases to amplify and solidify our data.

In summary, our study categorized the imaging of EGFR mutated NSCLC into 5 patterns. The diffuse intrapulmonary metastases pattern had worse clinical responses to TKI and other treatments. Patients with this imaging presentation were more likely to have their brain or leptomeningeal

involved, and also might contain less gene amplifications. This study helped to deepen our understanding of biological behavior of diffuse intrapulmonary metastases, and also argued for more aggressive treatment for these patients.

Data Sharing Statement

The datasets supporting the conclusions of this article are included within the article and partial data not shown.

Ethics Statement

The authors are accountable for all patient data accessed complied with relevant data protection and privacy regulations. This study was approved by the Ethics Committee on Biomedical Research, West China Hospital of Sichuan University (No. 2020-552). The informed consent was waived by the Ethics Committee on Biomedical Research, West China Hospital of Sichuan University, since this was a retrospective analysis.

Disclosure

The authors have no conflicts of interest to declare.

References

1. Bray F, Ferlay J, Soerjomataram I, et al. Global cancer statistics 2018: GLOBOCAN estimates of incidence and mortality worldwide for 36 cancers in 185 countries. *CA Cancer J Clin*. 2018;68 (6):394–424. doi:10.3322/caac.21492
2. E S K, Hirsh V, Mok T, et al. Gefitinib versus docetaxel in previously treated non-small-cell lung cancer (INTEREST): a randomised Phase III trial. *Lancet*. 2008;372(9652):1809–1818. doi:10.1016/S0140-6736(08)61758-4
3. Mitsudomi T, Morita S, Yatabe Y, et al. Gefitinib versus cisplatin plus docetaxel in patients with non-small-cell lung cancer harbouring mutations of the epidermal growth factor receptor (WJTOG3405): an open label, randomised Phase 3 trial.. *Lancet Oncol*. 2010;11 (2):104–105. doi:10.1016/S1470-2045(09)70364-X
4. Maemondo M, Inoue A, Kobayashi K, et al. Gefitinib or chemotherapy for non-small-cell lung cancer with mutated EGFR. *N Engl J Med*. 2010;362(25):2380–2388. doi:10.1056/NEJMoa0909530
5. Song J, Shi J, Dong D, et al. A New Approach to Predict Progression-free Survival in Stage IV EGFR-mutant NSCLC Patients with EGFR-TKI Therapy. *Clin Cancer Res*. 2018;24 (15):3583–3592. doi:10.1158/1078-0432.CCR-17-2507
6. Lee CK, Wu YL, Ding PN, et al. Impact of Specific Epidermal Growth Factor Receptor (EGFR) Mutations and Clinical Characteristics on Outcomes After Treatment With EGFR Tyrosine Kinase Inhibitors Versus Chemotherapy in EGFR-Mutant Lung Cancer: A Meta-Analysis. *J Clin Oncol*. 2015;33(17):1958–1965. doi:10.1200/JCO.2014.58.1736
7. Okuma Y, Kashima J, Watanabe K, et al. Survival analysis and pathological features of advanced non-small cell lung cancer with miliary pulmonary metastases in patients harboring epidermal growth factor receptor mutations. *J CANCER RES CLIN*. 2018;144 (8):1601–1611. doi:10.1007/s00432-018-2681-x
8. H J K, Kang SH, Chung HW, et al. Clinical features of lung adenocarcinomas with epidermal growth factor receptor mutations and miliary disseminated carcinomatosis. *Thoracic Cancer*. 2015;6 (5):629–635. doi:10.1111/1759-7714.12234
9. Togashi Y, Masago K, Kubo T, et al. Association of diffuse, random pulmonary metastases, including miliary metastases, with epidermal growth factor receptor mutations in lung adenocarcinoma. *Cancer*. 2011;117(4):819–825. doi:10.1002/cncr.25618
10. Zhao J, Dinkel J, Warth A, et al. CT characteristics in pulmonary adenocarcinoma with epidermal growth factor receptor mutation. *PLoS One*. 2017;12(9):e0182741. doi:10.1371/journal.pone.0182741
11. Hsu F, Nichol A, Toriumi T, et al. Miliary metastases are associated with epidermal growth factor receptor mutations in non-small cell lung cancer: a population-based study. *Acta Oncol*. 2017;56 (9):1175–1180. doi:10.1080/0284186X.2017.1328128

12. Gaikwad A, Souza CA, Inacio JR, et al. Aerogenous metastases: a potential game changer in the diagnosis and management of primary lung adenocarcinoma. *Am J Roentgenol*. 2014;203(6):W570–82. doi:10.2214/AJR.13.12088
13. Li R, Li X, Xue R, et al. Early metastasis detected in patients with multifocal pulmonary ground-glass opacities (GGOs). *Thorax*. 2018;73(3):290–292. doi:10.1136/thoraxjnl-2017-210169
14. Wu SG, Hu FC, Chang YL, et al. Frequent EGFR mutations in non-small cell lung cancer presenting with miliary intrapulmonary carcinomatosis. *Eur Respir J*. 2013;41(2):417–424. doi:10.1183/09031936.00006912
15. Cheng H, Perez-Soler R. Leptomeningeal metastases in non-small-cell lung cancer. *Lancet Oncol*. 2018;19(1):e43–e55. doi:10.1016/S1470-2045(17)30689-7
16. Yuan R, Yamada A, Weber B, et al. Radiographic patterns and survival of patients with early and late brain metastases in EGFR wild type and mutant non small cell lung cancer. *J Neuro-Oncol*. 2016;127(3):525–533. doi:10.1007/s11060-016-2057-5
17. Kurihara M, Koda H, Aono H, et al. Rapidly progressive miliary brain metastasis of lung cancer after EGFR tyrosine kinase inhibitor discontinuation: an autopsy report. *Neuropathology*. 2019;39 (2):147–155. doi:10.1111/neup.12542
18. Wu YL, Zhao Q, Deng L, et al. Leptomeningeal metastasis after effective first-generation EGFR TKI treatment of advanced non-small cell lung cancer. *Lung Cancer*. 2019;127:1–5. doi:10.1016/j.lungcan.2018.11.022
19. Nakamura Y, Takahashi T, Tsuya A, et al. Prognostic Factors and Clinical Outcome of Patients with Lung Adenocarcinoma with Carcinomatous Meningitis. *Anticancer Res*. 2012;32(5):1811–1816.
20. Pillai S, Khan A, Khan S. Adenocarcinoma of the Lung Presenting with Intrapulmonary Miliary Metastasis. *Cureus*. 2019;11(8):e5430.
21. Hoffman SA, Manski S, Deepak J. Miliary pattern on chest imaging as a presentation of EGFR-negative primary lung adenocarcinoma. *BMJ Case Rep*. 2019;12(5):5. doi:10.1136/bcr-2018-228534
22. Jacob M, Freitas C, Fernandes G. Lung adenocarcinoma with miliary metastases mimicking disseminated tuberculosis. *Jpn J Clin Oncol*. 2019;49(9):888–889. doi:10.1093/jjco/hyz107
23. Sekine A, Katano T, Oda T, et al. Miliary lung metastases from non-small cell lung cancer with Exon 20 insertion: A dismal prognostic entity: A case report. *Mol Clin Oncol*. 2018;9(6):673–676. doi:10.3892/mco.2018.1730
24. Patil T, Pacheco JM. Miliary Metastases in Non–Small-Cell Lung Cancer. *N Engl J Med*. 2018;379(20):1945. doi:10.1056/NEJMicm1803514
25. Schaller A, Beau-Faller M, Mennecier B, et al. Lung Adenocarcinoma with Pulmonary Miliary Metastases and Complex Somatic Heterozygous EGFR Mutation. *Case Rep Oncol*. 2014;7 (3):769–773. doi:10.1159/000369526
26. Poonia S, Berge EM, Aisner DL, et al. EGFR exon 19 deletion mutations and systemic/central nervous system miliary metastasis: clinical correlations and response to therapy. *Clin Lung Cancer*. 2014;15(5):387–389. doi:10.1016/j.cllc.2014.04.005
27. Lim CK. The Moth-Eaten Lung: lung Adenocarcinoma with Cavitating Miliary Intrapulmonary Carcinomatosis. *J Thorac Oncol*. 2015;10(9):1375. doi:10.1097/JTO.0000000000000542
28. Falk AT, Poudenx M, Otto J, et al. Adenocarcinoma of the lung with miliary brain and pulmonary metastases with echinoderm microtubule-associated protein like 4-anaplastic lymphoma kinase translocation treated with crizotinib: A case report. *Lung Cancer*. 2012;78(3):282–284. doi:10.1016/j.lungcan.2012.08.015
29. Inomata M, Hayashi R, Kenta K, et al. Miliary brain metastasis presenting with calcification in a patient with lung cancer: a case report. *J Med Case Rep*. 2012;6(1):279. doi:10.1186/1752-1947-6-279
30. Mochizuki S, Nishimura N, Inoue A, et al. Miliary brain metastases in 2 cases with advanced non-small cell lung cancer harboring EGFR mutation during gefitinib treatment. *Respir Investig*. 2012;50 (3):117–121. doi:10.1016/j.resinv.2012.06.002

31. Ogawa M, Kurahashi K, Ebina A, et al. Miliary brain metastasis presenting with dementia: progression pattern of cancer metastases in the cerebral cortex. *Neuropathology*. 2007;27(4):390–395. doi:10.11 11/j.1440-1789.2007.00782.x

32. Laack E, Simon R, Regier M, et al. Miliary never-smoking adenocarcinoma of the lung: strong association with epidermal growth factor receptor exon 19 deletion. *J Thorac Oncol*. 2011;6 (1):199–202. doi:10.1097/JTO.0b013e3181fb7cf1

33. A M R, Stankoff B, Lavole A, et al. Miliary Brain Metastases in Lung Cancer. *J Clin Oncol*. 2010;28(34):e714–6. doi:10.1200/JCO.2009.27.0140

34. Zhao J, Lin G, Zhuo M, et al. Next-generation sequencing based mutation profiling reveals heterogeneity of clinical response and resistance to osimertinib. *Lung Cancer*. 2020;141:114–118. doi:10.1016/j.lungcan.2019.10.021

35. Lai GGY, Lim TH, Lim J, et al. Clonal MET Amplification as a Determinant of Tyrosine Kinase Inhibitor Resistance in Epidermal Growth Factor Receptor-Mutant Non-Small-Cell Lung Cancer. *J Clin Oncol*. 2019;37(11):876–884. doi:10.1200/JCO.18.00177

36. Lee CK, Man J, Lord S, et al. Checkpoint Inhibitors in Metastatic EGFR- Mutated Non–Small Cell Lung Cancer—A Meta-Analysis. *J Thorac Oncol*. 2017;12(2):403–407. doi:10.1016/j.jtho.2016.10.007

37. Yamada T, Hirai S, Katayama Y, et al. Retrospective efficacy analysis of immune checkpoint inhibitors in patients with EGFR-mutated non-small cell lung cancer. *Cancer Med*. 2019;8(4):1521–1529. doi:10.1002/cam4.2037

38. Lisberg A, Cummings A, J W G, et al. A Phase II Study of Pembrolizumab in EGFR-Mutant, PD-L1+, Tyrosine Kinase Inhibitor negative Patients With Advanced NSCLC. *J Thorac Oncol*. 2018;13(8):1138–1145. doi:10.1016/j.jtho.2018.03.035